Journal of Power Sources 196 (2011) 1242–1247

Contents lists available at ScienceDirect

Journal of Power Sources

journal homepage: www.elsevier.com/locate/jpowsour

Preparation of fibrous Ni-coated-YSZ anodes for solid oxide fuel cells

Luping Li, Peigen Zhang, Ranran Liu, S.M. Guo*

Department of Mechanical Engineering, Louisiana State University, Baton Rouge, LA 70803, USA

ARTICLE INFO

Article history:
Received 6 July 2010
Received in revised form 12 August 2010
Accepted 13 August 2010
Available online 19 August 2010

Keywords:
Electrospinning
Electroless Ni plating
SOFC anodes
Fiber-derived anodes

ABSTRACT

A novel route to fabricate nanofiber-derived low-Ni-content anodes for solid oxide fuel cells (SOFCs) is presented. Uniform YSZ nanofibers were first synthesized by electrospinning of 8YSZ dispersion; the fiber surfaces were then electrolessly plated with a layer of Ni after sintering of the electrospun fibers. The Ni-YSZ nanofibers were slurry coated as the anode onto a commercial half cell that was subsequently tested. The deposited anode was found to have a Ni loading of 30 wt%, a value well below the conventional percolation threshold. A second cell with the same Ni content in the anode, prepared by conventional ball-milling of individual powders, was also fabricated and tested. We found that the peak power density for the cell with the fiber-derived anode is twice of that with the powder-derived anode, which was attributed to the former's larger TPB sites.

1. Introduction

A solid oxide fuel cell (SOFC) is a ceramic electrochemical device that converts chemical energy directly into electrical energy. For decades, SOFCs stayed at the center of research primarily due to their high efficiency in energy conversions (40–60% unassisted, up to 70% in pressurized hybrid system) compared to engines and modern thermal power plants (30–40% efficient) [1]. SOFCs have other advantages such as environmental friendliness, diversity of fuels that can be used, reliability of power generation, etc.

Ni-YSZ cermet is the state-of-the-art material for SOFC anodes [2,3]. In the composite, Ni acts both as a catalyst for electrochemical reaction and as an electron conductor; the YSZ forms a matrix for Ni dispersion to prevent Ni coarsening under operating conditions. YSZ also plays the role of transporting ions within the anode.

It is well established that contiguous Ni–Ni chain has to be established within the anode [4] to reduce the ohmic resistance and to achieve the percolation threshold, which requires sufficient Ni amount be present; on the other hand, because the thermal expansion coefficient (TEC) of Ni is much higher than that of YSZ, too much Ni will result in poor structural integrity of the cell. To overcome this dilemma, many research efforts are focused on investigating the processing-microstructure-property relations of the anode and tailoring its morphologies [5]. Various methods have been used to fabricate SOFC anodes, including mechanical mixing [6], atmospheric plasma spray (APS) [7], tape casting [8], combustion synthesis [9], co-precipitation [10], etc. Most of these techniques targeted uniform distribution of Ni particles in YSZ matrix and the current Ni percolation threshold is essentially above 44.38 wt% [11].

In this work, we attempted to construct a novel nanofiber-derived anode by using Ni-coated YSZ nanofibers. The primary objective was to examine the effectiveness of the fibrous anode in terms of microstructure and cell performance, based on a Ni content (30 wt%) well below the current Ni percolation threshold, with the hope of reducing the threshold by utilizing this new anode structure.

2. Experimental

2.1. 8YSZ nanofiber preparation

Electrospinning is versatile technique that can be used to fabricate uniform fibers [12]. The 8YSZ nanofibers were fabricated by electrospinning using an electrospinning rig described in our previous work [13]. Colloidal yttria (14 wt%) and zirconia (acetate stabilized, 20 wt%) were purchased from Nyacol Nano-Technologies, Inc., USA and the as-received particle sizes were ~10 nm for both dispersions. The two suspensions were weighed and mixed to give the stoichiometry of 8YSZ, which was then added to polyvinylpyrrolidone (PVP)/ethanol solution. To ensure homogeneity, the precursor was further mixed in an ultrasonic bath and subsequently loaded onto the electrospinning rig. A voltage of 6.2 kV was imposed between the syringe needle and the collector,

* Corresponding author. Tel.: +1 225 578 7619; fax: +1 225 578 5924.
E-mail address: sguo2@lsu.edu (S.M. Guo).

0378-7753/$ – see front matter © 2010 Elsevier B.V. All rights reserved.
doi:10.1016/j.jpowsour.2010.08.038

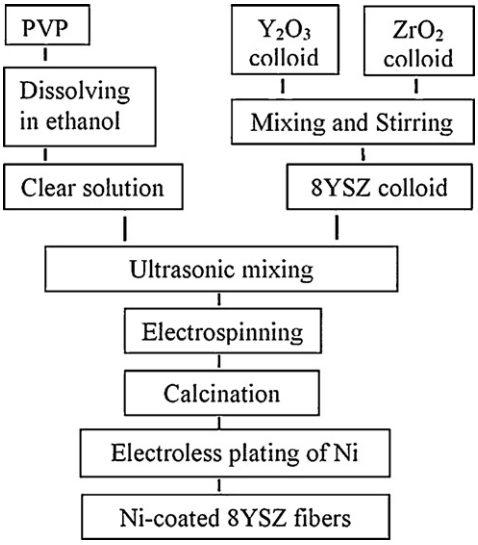

Fig. 1. Flow chart illustrating the preparation of Ni-coated 8YSZ nanofibers.

which was a piece of alumina foil. The major sample-preparation steps, including Ni plating to be presented in Section 2.2, are summarized in Fig. 1.

2.2. Ni plating on YSZ nanofibers

The as-spun fibers were sintered at 1000 °C for 3 h to remove the organics. Prior to coating, the fibers were sensitized and activized by soaking them in acidified $SnCl_2$ and $PdCl_2$ hydrosols, respectively. Similar pre-treating processes were also used by other authors [2,14]. The treated fibers were then baked off overnight at 80 °C in a furnace. Ni plating was conducted at temperatures between 60 and 65 °C using a water bath/hot plate arrangement. The fibers were loaded into a coating solution, which was derived from Wen et al.'s work [15]. The composition of the coating solution exploited in this study was presented in Table 1.

Table 1
The composition of the Ni plating solution used in this study.

$Ni(AC)_2$	50 g L^{-1}
EDTA	20 g L^{-1}
Lactic acid	40 mL L^{-1}
N_2H_4	80 mL L^{-1}
NaOH	35 g L^{-1}

The fibers were characterized by powder X-ray Diffraction (XRD) (Bruker/Siemens D5000 X-ray diffractometer with Rietveld software), and field emission scanning electron microscopy (FESEM) (Quanta 3D FEG, FEI Company, USA).

2.3. Deposition of the Ni-YSZ fibers onto half cells

A slurry-coating method was used to deposit Ni-YSZ fibers as the anode onto a commercial single-electrode SOFC cell (NexTech Materials, Ohio, USA), which had electrolyte and cathode side only. The diameter of the 8YSZ supporting electrolyte is 20 mm and the LSM cathode is 12.5 mm, which is used to calculate the effective area of the cell. To prepare the anode, the Ni-YSZ fibers were first fired to 500 °C to remove the organics introduced during Ni plating. Then the fibers were ground briefly using an agate mortar. An organic solvent system for slurry coating was made by mixing methyl ethyl ketone (MEK) and ethanol at a 1:1 weight ratio, with the addition of polyvinyl butyral (PVB) as the binder and fish oil as the dispersant. The fibers were added into the solvent system and were mixed to form homogeneous slurry. Finally the slurry was deposited onto the commercial half cell to form a complete button cell. After drying in air for 2 h, the coated cell was transferred into

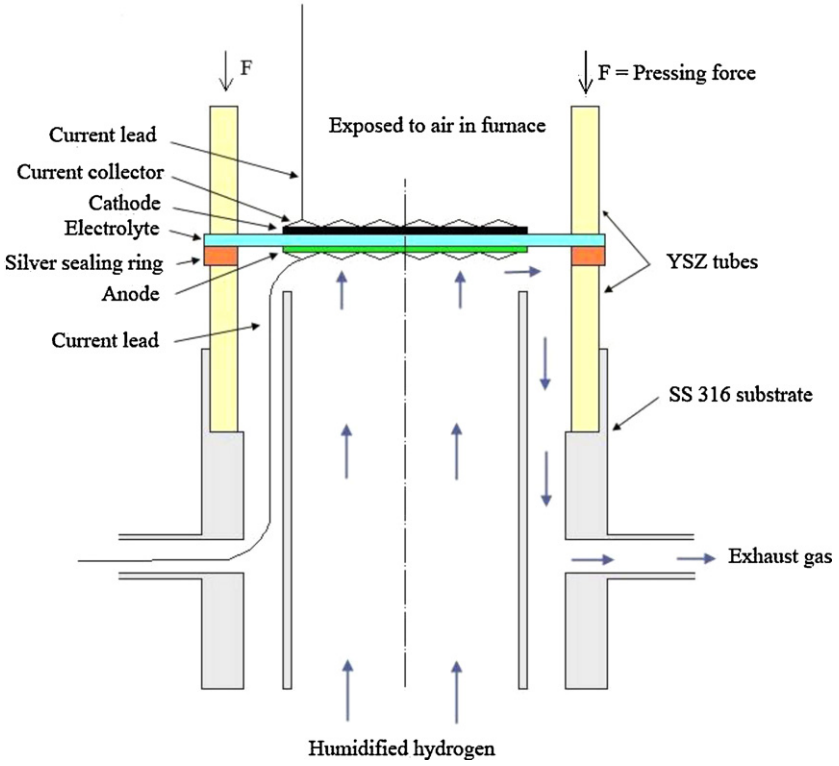

Fig. 2. Schematic of the fuel cell testing rig.

a furnace and was fired to 1300 °C for 1 h with temperature ramp of 3 °C min^{-1}.

In order to determine the Ni concentration in the anode, X-ray photoelectron spectroscopy (XPS) (model AXIS 165, Kratos Analytical, Japan) was used. Quantification was conducted based on the area of each element's high-resolution spectrum obtained. It was found that there was 30 wt% of Ni in the anode composite.

To evaluate and to compare the fiber-derived anode with the "conventional" anode in terms of microstructure and cell performance, a powder-derived anode was developed on a second half cell using a similar slurry-coating technique: NiO powder (Sigma–Aldrich, USA, particle size <50 nm) and YSZ powder (TZ-8Y, Tosoh Corp., Japan) were weighed and mixed to give the same Ni content (30 wt%). The NiO-YSZ mixture was ball-milled and was coated on the second half cell. Finally the cell was calcined using the same temperature program.

2.4. Cell testing

After sintering of the newly applied anodes, gold ink (NexTech Materials, Ohio, USA) was used to attach gold meshes (Alfa Aesar, USA) to both sides of the cell. "Two-probe" testing method was employed in this study and gold electrical wires were used. The cell was installed on a home-made testing stand, as shown in Fig. 2. Silver rings were cut from a silver sheet (A.D. Mackay, Inc., USA, 99.95% purity, 0.254 mm thickness) and were used for sealing between the cell and the testing stand. Cell performance was tested between 650 and 800 °C. During testing bubbled hydrogen was maintained at 90 mL min^{-1} and cathode side was exposed to the static air in the furnace.

3. Results and discussion

3.1. FESEM characterizations of fibers

Fig. 3(a) and (b) shows the FESEM image of the as-spun nanofibers. It can be noted that uniform, defect-free YSZ fibers were fabricated on a large scale; the diameters of these fibers are ~300 nm and fiber surfaces are smooth.

After sinteration at 1000 °C (see Fig. 4(a)), fiber's surface morphology went through dramatic changes: the surfaces became much rougher and large grains are clearly seen. This phenomenon is classically called "thermal grooving" [16] and is attributed to particles' surface diffusion, which was explained in our previous work [13]. Fig. 4(b) shows the fibers after Ni coating. Ni additions on fiber surfaces can be noted easily when compared to

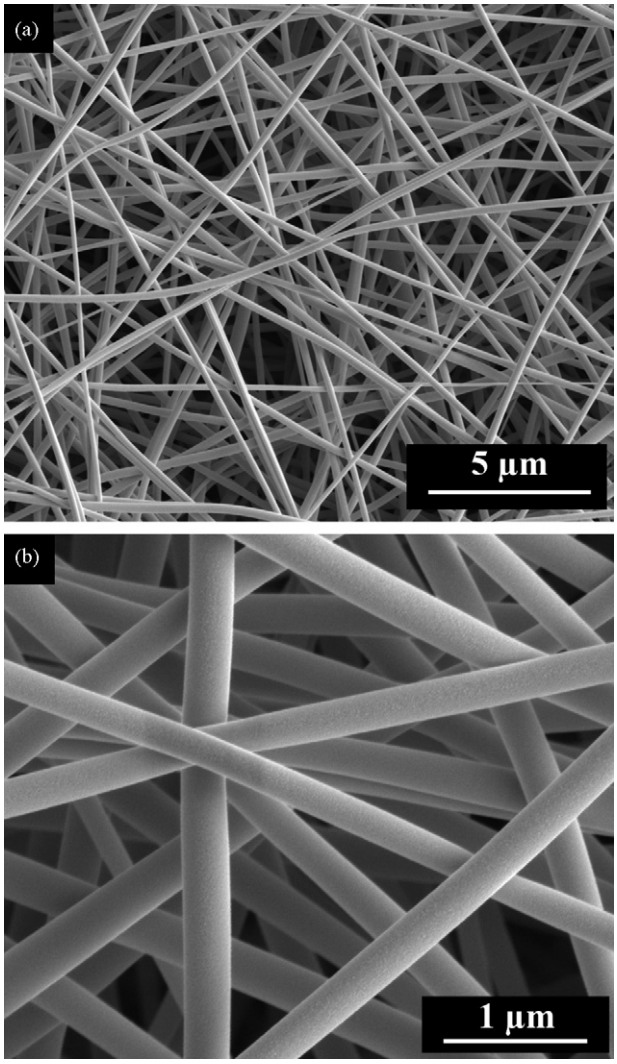

Fig. 3. FESEM graphs of the as-spun YSZ fibers.

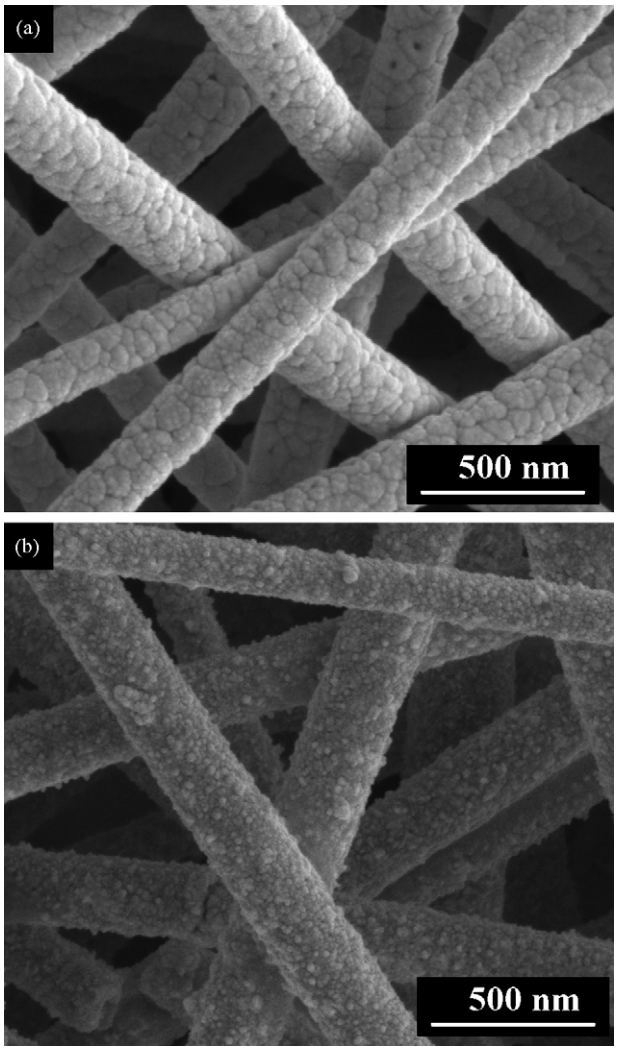

Fig. 4. FESEM images of the nanofibers: (a) after sinteration and (b) after Ni coating.

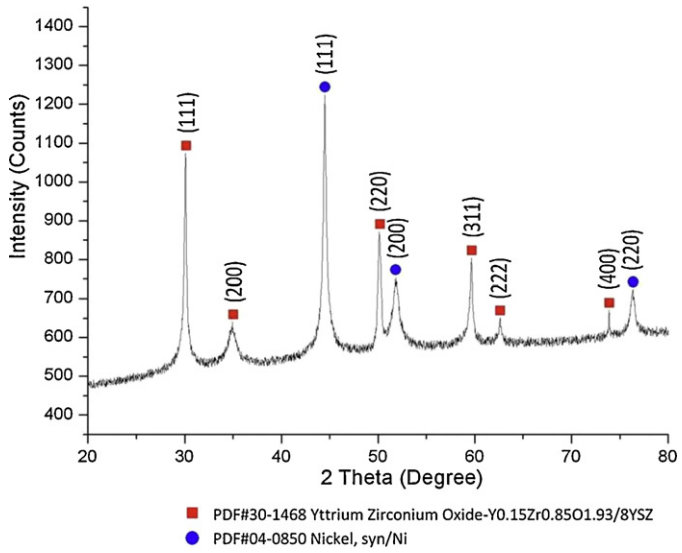

Fig. 5. XRD pattern of the Ni coated YSZ fibers.

Fig. 4(a). No major defects for the coating are present, such as Ni agglomeration, spallation or separation, which were reported by other authors [2,15]. It should also be emphasized that in Fig. 4(b) fine Ni particles distributed evenly and uniformly, leading to the establishment of adjoining and connected Ni–Ni chains on fiber surfaces.

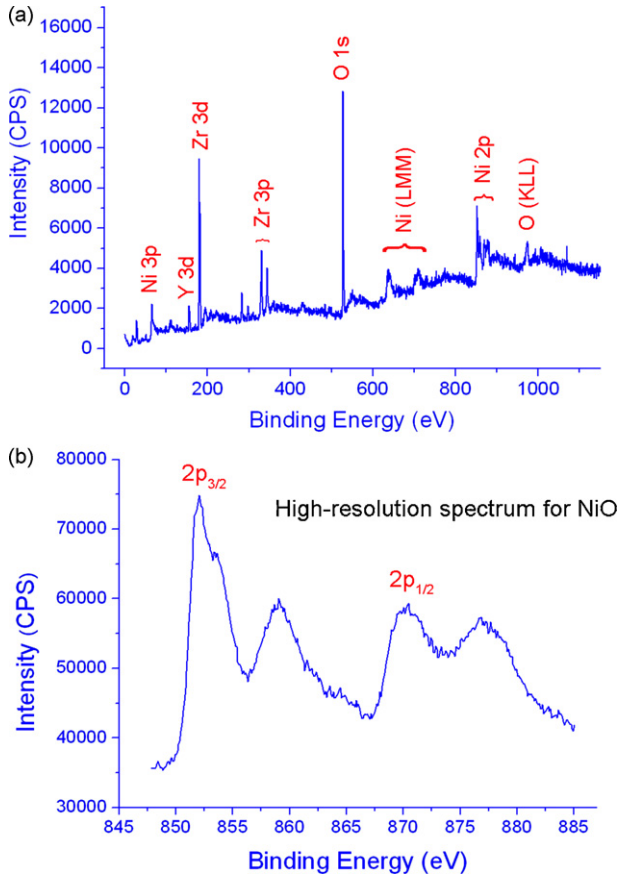

Fig. 6. XPS spectra of the fiber-derived anode after cofiring: (a) wide-scan survey spectrum and (b) high-resolution spectrum for NiO.

3.2. Compositional characterizations

The Ni-coated fibers were examined by XRD and the results are shown in Fig. 5. We found that the 8YSZ had a cubic crystalline structure with a lattice parameter of 5.139 Å, which is in agreement with the reported value in the literature [17]. The coated Ni had a hexagonal crystalline structure rather than being amorphous, which was often the case in Ni-P and Ni-B electroless plating processes [18].

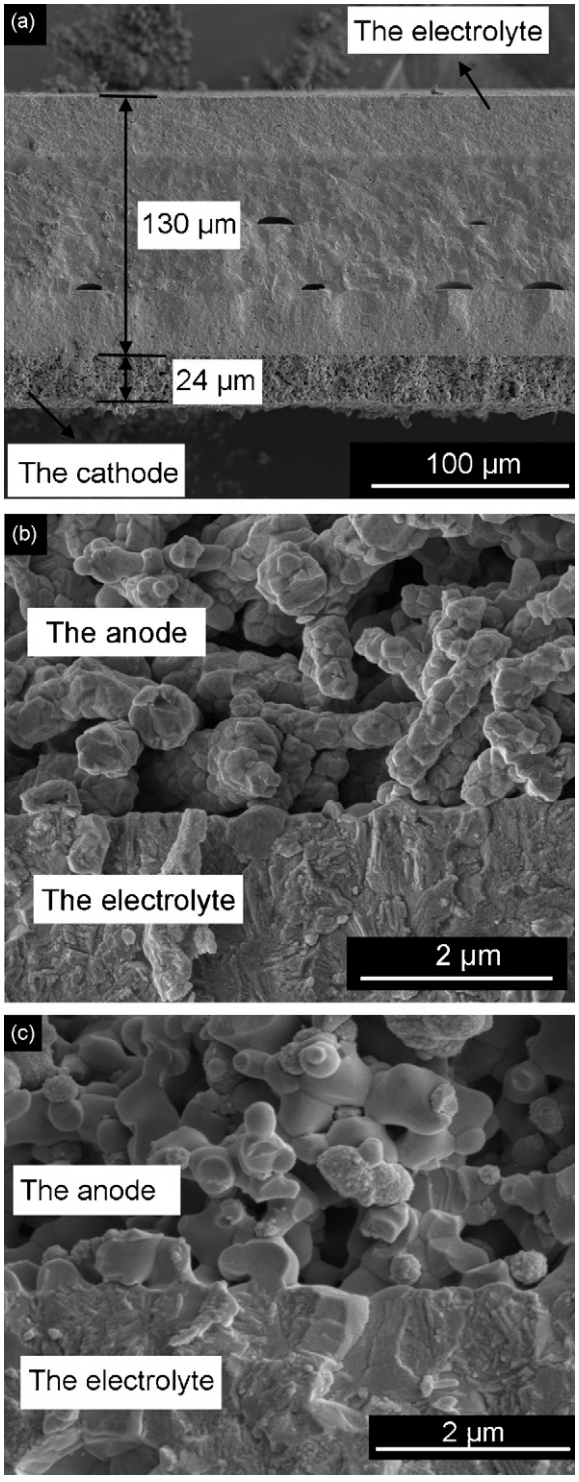

Fig. 7. FESEM images of the cross-sections of (a) the as-received half cell, (b) the fiber-derived anode, and (c) the powder-derived anode.

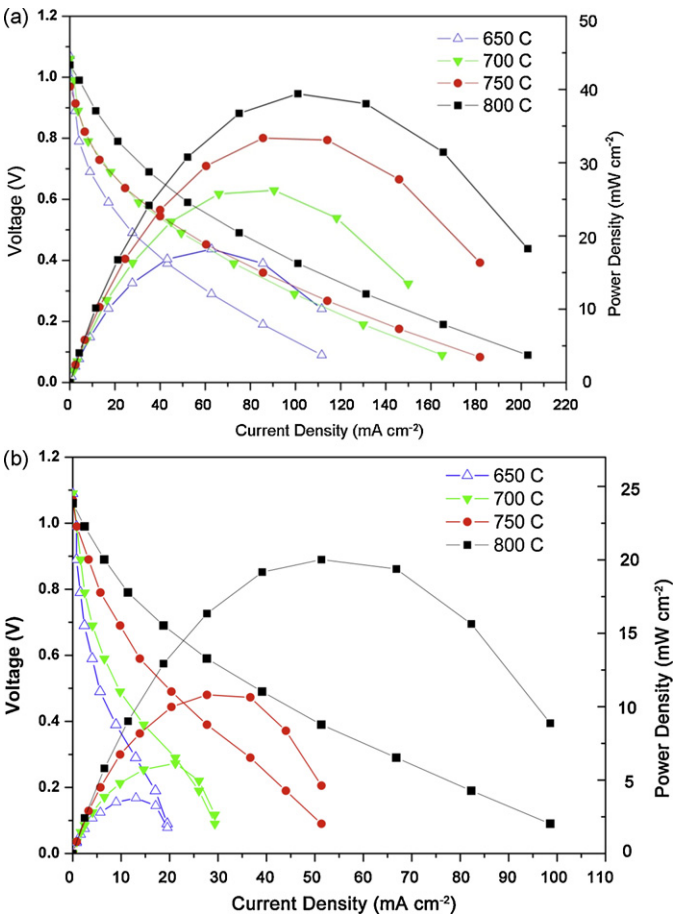

Fig. 8. Comparison of the performance of two SOFC button cells, both having 30 wt% of Ni in the anode: (a) fiber-derived anode and (b) conventional powder-derived anode.

Fig. 6(a) shows the wide-scan survey spectrum for all elements that present in the fiber-derived anode. Fig. 6(b) is the sample's typical high-resolution spectrum for NiO. It should be noted that at this stage after sinteration of the anode, the electroless-plated Ni had been oxidized to NiO, which will be reduced to Ni by hydrogen during cell's initial operations. It was determined by XPS that there was 30 wt% of Ni present in the anode.

3.3. FESEM examinations and cell performance

In order to examine the microstructure of the cells, the as-received half cell, together with the fiber-derived and the powder-derived cell were fractured after testing and the cross-sections were examined by FESEM. The results are shown in Fig. 7. The thickness of the cathode and the electrolyte layer of the as-received half cell (see Fig. 7(a)) is 24 and 130 μm, respectively. When comparing the anode structure in Fig. 7(b) (fiber-derived cell) with (c) (powder-derived cell), it is evident that the fiber-derived anode mainly consisted of nanofibers, which formed an interconnected network within the anode; on the other hand, the particles in the powder-derived anode formed sphere-like granules that were unorganized and were not well-connected, which are not favorable for the anode functionality under Ni content of only 30 wt%.

The *I–V* curves of the two cells both having 30 wt% of Ni in the anode are shown in Fig. 8(a) and (b). It can be noted that the cells generally performed better at higher temperatures. The power density of the fiber-derived cell is dramatically higher than that of the powder-derived one over the entire temperature range tested. The peak power density, which was reached at 800 °C, was 40 and 20 mW cm^{-2} for the fiber-derived cell (Fig. 8(a)) and the powder-derived cell (b), respectively. Because of the identical Ni amount used, it is reasonable to attribute the variation in performance between the two cells to the different anode structures that were dictated by the two different preparation approaches. The effectiveness of the fibrous anode structure containing 30 wt% of Ni is thus apparent.

3.4. Further discussion

Although this work is performed with Ni loading far below the traditional percolation threshold (44.38 wt% [11]), which will cause limited number of interconnected electron conducting pathways, the fibrous Ni-coated YSZ anodes clearly showed advantages over the powder-derived counterpart.

The fiber-derived structure not only provides continuous and smooth ion path along the YSZ core of the fibers, it also promotes good electron conduction in the Ni layer on the fiber surfaces. Additionally, the spacing between the fibers will greatly facilitate gas diffusion. In short, in the fiber-derived anode structure, an enlarged three-phase-boundary (TPB) [4] network is formed in 3D space and thus it has led to enhanced cell performance. Additionally, because of the uniform distribution of Ni as thin layers on YSZ fiber surfaces, reduced Ni percolation threshold can be expected, which will enhance cells' structural integrity and long-term stability [19,20] due to less Ni usage required to establish sound electron conduction.

4. Conclusions

8YSZ nanofibers were fabricated using electrospinning and the fiber surfaces were successfully plated with Ni by an electroless plating technique. The Ni-YSZ fibers were slurry coated on a commercial half cell as the anode and the cell performance was tested. The Ni concentration in the anode was found to be 30 wt% by XPS technique. To compared the novel fibrous anode structure with conventional powder-derived anode, a second cell with the same Ni content in the anode was prepared by mixing Ni and YSZ powders using ball-milling and subsequent slurry coating on another half cell. The peak power density of the cell with fiber-derived anode was found to be twice of that with the powder-derived anode. The better performance was attributed to the well-structured, interconnected fibers in the fiber-derived anode.

Acknowledgements

This work was supported by Louisiana Board of Regents under contract LEQSF (2007-10)-RD-A-08; the authors are indebted to Dr. Dongmei Cao for help with FESEM operations.

References

[1] S.C. Singhal, Solid State Ionics 135 (2000) 305.
[2] S.K. Pratihar, A. Das Sharma, R.N. Basu, H.S. Maiti, J. Power Sources 129 (2004) 138–142.
[3] S.-D. Kim, H. Moon, S.-H. Hyun, J. Moon, H. Kim, H.-W. Lee, Solid State Ionics 177 (2006) 931.
[4] J.R. Wilson, W. Kobsiriphat, R. Mendoza, H.-Y. Chen, J.M. Hiller, D.J. Miller, K. Thornton, P.W. Voorhees, S.B. Adler, S.A. Barnett, Nat. Mater. 5 (2006) 541.
[5] S. Kima, O. Kwona, S.K. Yuming Xionga, C. Lee, Surf. Coat. Technol. 202 (2008) 3180.
[6] T. Fukui, K. Murata, S. Ohara, H. Abe, M. Naito, K. Nogi, J. Power Sources 125 (2004) 17.
[7] G. Kim, H. Choi, C. Han, S. Uhm, C. Lee, Surf. Coat. Technol. 195 (2005) 107.
[8] J.-H. Song, N.M. Sammes, S.-II. Park, S. Boo, H.-S. Kim, H. Moon, S.-H. Hyun, J. Fuel Cell Sci. Technol. 5 (2008) 021003.
[9] A. Ringuede, J.A. Bronine, J.R. Frade, Solid State Ionics 146 (2002) 219.

[10] S. Mosch, N. Trofimenko, M. Kusnezoff, T. Betz, M. Kellner, Solid State Ionics 179 (2008) 1606.
[11] S.K. Pratihar, A.D. Sharma, H.S. Maiti, Mater. Chem. Phys. 96 (2006) 388.
[12] R. Bajon, S. Balaji, S.M. Guo, J. Fuel Cell Sci. Technol. 6 (2009) 031004.
[13] L. Li, P. Zhang, J. Liang, S.M. Guo, Ceram. Int. 36 (2010) 589.
[14] T. Ignatius, R.S. Smith, US patent 3,212,917 (1962).
[15] G. Wen, Z.X. Guo, C.K.L. Davies, Scr. Mater. 43 (2000) 307.
[16] W.W. Mullins, J. Appl. Phys. 28 (1957) 333.
[17] V. Esposito, D.Z. de Florio, F.C. Fonseca, E.N.S. Muccillo, R. Muccillo, E. Traversa, J. Eur. Ceram. Soc. 25 (2005) 2637–2641.
[18] K.H. Yoon, H.S. Park, S.O. Yoon, H.I. Song, J. Mater. Sci. Lett. 8 (1989) 1442.
[19] M. Marinsek, K. Zupan, J. Macek, J. Power Sources 86 (2000) 383.
[20] M. Lang, T. Franco, G. Schiller, N. Wagner, J. Appl. Electrochem. 32 (2002) 871.